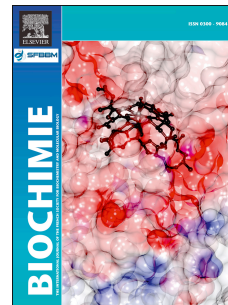# Journal Pre-proof

Conformational analysis and *in vitro* immunomodulatory and insulinotropic properties of the frog skin host-defense peptide rhinophrynin-27 and selected analogs

Mariano A. Scorciapino, Paola Carta, Jelena Pantic, Miodrag L. Lukic, Aleksandra Lukic, Vishal Musale, Yasser H.A. Abdel-Wahab, J. Michael Conlon

Please cite this article as: M.A. Scorciapino, P. Carta, J. Pantic, M.L. Lukic, A. Lukic, V. Musale, Y.H.A. Abdel-Wahab, J.M. Conlon, Conformational analysis and *in vitro* immunomodulatory and insulinotropic properties of the frog skin host-defense peptide rhinophrynin-27 and selected analogs, *Biochimie*, https://doi.org/10.1016/j.biochi.2019.10.007.

This is a PDF file of an article that has undergone enhancements after acceptance, such as the addition of a cover page and metadata, and formatting for readability, but it is not yet the definitive version of record. This version will undergo additional copyediting, typesetting and review before it is published in its final form, but we are providing this version to give early visibility of the article. Please note that, during the production process, errors may be discovered which could affect the content, and all legal disclaimers that apply to the journal pertain.

E-13

RP-27 in 50% TFE-water
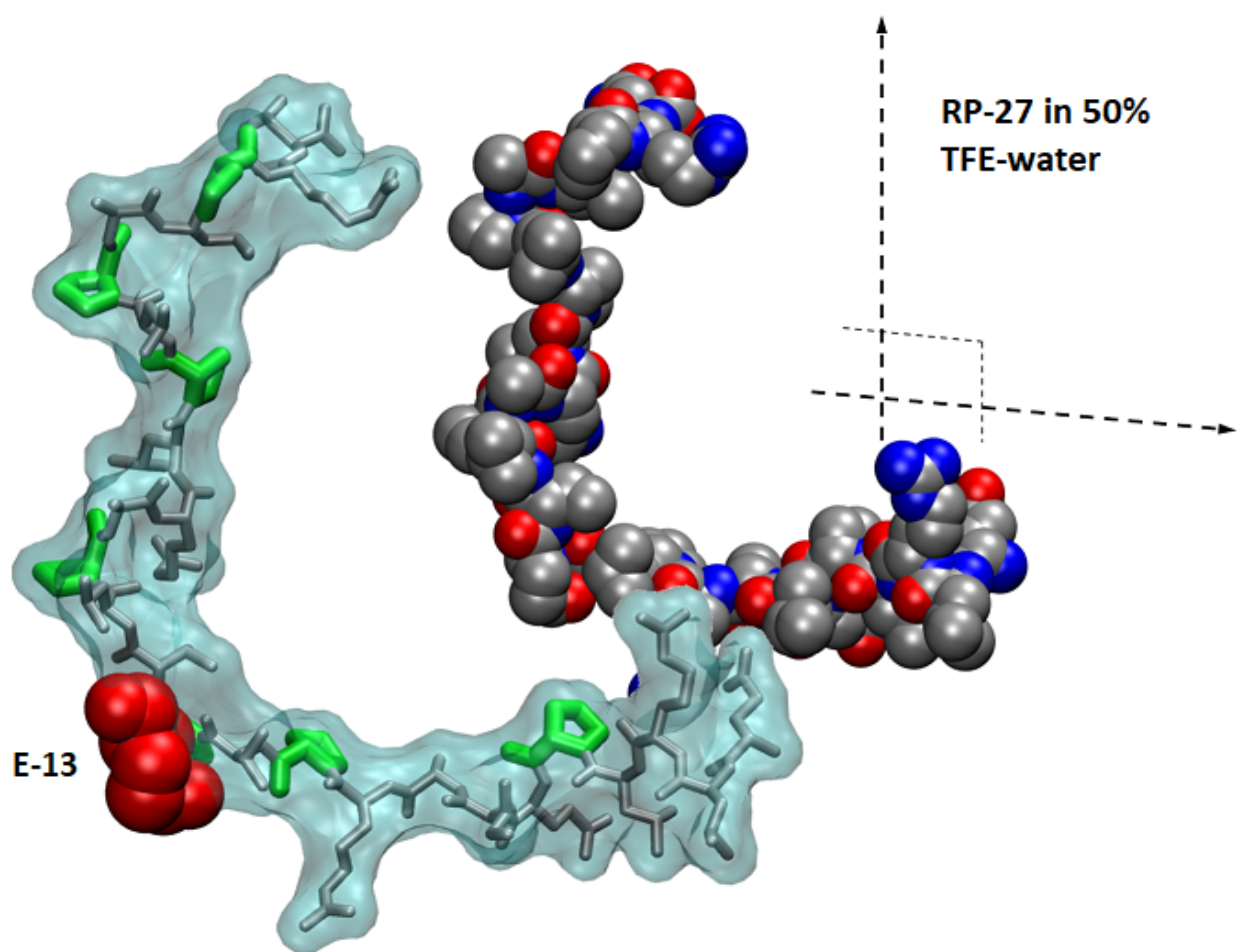
Conformational analysis and *in vitro* immunomodulatory and insulinotropic properties of the frog skin host-defense peptide rhinophrynin-27 and selected analogs

Mariano A. Scorciapino[a], Paola Carta[a], Jelena Pantic[b], Miodrag L. Lukic[c], Aleksandra Lukic[c], Vishal Musale[d] , Yasser H.A. Abdel-Wahab[d], J. Michael Conlon[d]*

[a]*Department of Chemical and Geological Sciences, University of Cagliari, Cagliari, Italy.*

[b]*Center for Molecular Medicine and Stem Cell Research, Faculty of Medical Sciences, University of Kragujevac, Kragujevac, Serbia*

[c]*Department of Endodontics, Faculty of Medical Sciences, University of Kragujevac, Kragujevac, Serbia.*

[d]*Diabetes Research Group, School of Biomedical Sciences, Ulster University, Coleraine BT52 1SA, N. Ireland, U.K.*

[*]**Correspondence**

J. Michael Conlon, Diabetes Research Group, School of Biomedical Sciences, Ulster University, Cromore Rd, Coleraine BT52 1SA, N. Ireland, U.K.

E-mail: m.conlon@ulster.ac.uk   Tel: 44-7918526277

ABSTRACT

The study investigates conformational analysis and the *in vitro* cytokine-mediated immunomodulatory and insulin-releasing activities of rhinophrynin-27 (ELRLPEIARPVPEVLPARLPLPALPRN; RP-27), a proline-arginine-rich peptide first isolated from skin secretions of the Mexican burrowing toad *Rhinophrynus dorsalis* (Rhinophrynidae). In both water and 50% trifluoroethanol-water, the peptide adopts a polyproline type II helical conformation with a high degree of deviation from the canonical collagen-like folding and a pronounced bend in the molecule at the Glu^{13} residue. Incubation of mouse peritoneal cells with RP-27 significantly ($P < 0.05$) inhibited production of the pro-inflammatory cytokines TNF-α and IL-1β and stimulated production of the anti-inflammatory cytokine IL-10. The peptide significantly ($P < 0.01$) stimulated release of insulin from BRIN-BD11 rat clonal β-cells at concentrations ≥ 1 nM while maintaining the integrity of the plasma membrane and also stimulated insulin release from isolated mouse islets at a concentration of 10^{-6} M. Increasing the cationicity of RP-27 by substituting glutamic acid residues in the peptide by arginine and increasing hydrophobicity by substituting alanine residues by tryptophan did not result in analogues with increased activity with respect to cytokine production and insulin release. The combination of immunosuppressive and insulinotropic activities together with very low cytotoxicity suggests that RP-27 may represent a template for the development of an agent for use in anti-inflammatory and Type 2 diabetes therapies.

Key words: Rhinophrynin-27; frog skin; cytokine; insulin release; Type 2 diabetes; anti-inflammatory

2

Abbreviations used

GLP-1: Glucagon-like peptide-1

GRAVY: Grand Average of Hydropathy

IL-1β: Interleukin-1β

IL-10: Interleukin-10

KRB: Krebs-Ringer bicarbonate buffer

LDH: Lactate dehydrogenase

RMSD: Root mean square deviation

RP-27: Rhinophrynin-27

RP-33: Rhinophrynin-33

T2DM: Type 2 diabetes mellitus

TFE: Trifluoroethanol

TNF-α: Tumor necrosis factor-alpha

TSP: Trimethylsilylpropanoic acid

1.   Introduction

The Mexican burrowing toad *Rhinophrynus dorsalis* is the sole extant representative of the Rhinophrynidae, a phylogenetically ancient family of frogs that is the sister-group to the more extensive Pipidae family [1]. Peptidomic analysis of norepinephrine-stimulated secretions from *R. dorsalis* led to the isolation of a proline-arginine-rich peptide, termed rhinophryinin-27 (RP-27) together with a C-terminally extended form termed rhinophrynin-33 (RP-33) [2]. RP-27 shows limited structural similarity to the porcine multifunctional peptide PR-39 [3] but, unlike this peptide, it displayed no growth-inhibitory activity against the Gram-positive *Staphylococcus epidermidis* and Gram-negative *Escherichia coli* bacteria and against the opportunistic yeast pathogen *Candida parapsilosis* (MIC > 128 μM) and lacked cytotoxic activity against mouse erythrocytes (LC_{50} > 500 μM) and A549 human non-small cell lung adenocarcinoma cells (LC_{50} > 100 μM) [2]. Circular dichroism studies suggested that RP-27 adopts a polyproline type II (PPII) helical structure in aqueous solution and a conformation composed of a PP-II helix and turn structures in the presence of sodium dodecyl sulphate micelles [2].

Many peptides that were first identified in frog skin secretions as a result of their antimicrobial activities and abilities to lyse mammalian cells have subsequently been shown to be multifunctional. Biological activities not directly linked to cytotoxicity include cytokine-mediated immunomodulatory properties [4], stimulation of insulin release from clonal β-cells and isolated pancreatic islets [5] and glucagon-like peptide-1 release from enteroendocrine cells [6] together with β-cell proliferative and anti-apoptotic [7], wound healing [8] and anti-oxidative [9] activities. The aim of the present study was three-fold: (1) to determine the conformation of the peptide in aqueous solution and membrane-mimetic media using ^{1}H-NMR spectroscopy, (2) to investigate its biological activities in order to

4

assess the potential for development into an agent with therapeutic relevance, and (3) to gain insight into the possible physiological role of the RP-27 in its species of origin. To these ends, the effects of incubation with synthetic RP-27, RP-33 and selected analogues with increased cationicity and increased hydrophobicity on the production of pro- and anti-inflammatory cytokines by mouse peritoneal cells and release of insulin from BRIN-BD11 rat clonal β-cells [10] were investigated.

2. Materials and methods

2.1. Peptides

RP-27, RP-33 and all analogues were supplied in crude form by Synpeptide Co., Ltd (Shanghai, China). The peptides were purified by reversed-phase HPLC on a (2.2 cm x 25 cm) Vydac 218TP1022 (C-18) column equilibrated with acetonitrile/ water/trifluoroacetic acid (28.0/71.9.9/0.1, v/v/v) at a flow rate of 6 mL/min. The concentration of acetonitrile was raised to 56 % (v/v) over 60 min using a linear gradient. Absorbance was measured at 214 nm and the major peak in the chromatogram was collected manually. The identities of the peptides were confirmed by electrospray mass spectrometry and their final purities were > 98%. The primary structures, calculated isoelectric points (pI) [11], and Grand Average of Hydropathy (GRAVY) calculated from the Wimley-White amino acid hydrophobicity scales [12] of the peptides used in this study are shown in Table 1.

5

Table 1. Primary structure and physicochemical properties of the rhinophrynin

peptides used in this study

		pI	GRAVY
RP-27	ELRLPEIARPVPEVLPARLPLPALPRN	10.72	-0.36
RP-33	ELRLPEIARPVPEVLPARLPLPALPRNKMAKNQ	11.36	-0.39
[E1R]RP-27	RLRLPEIARPVPEVLPARLPLPALPRN	11.66	-0.32
[E1R,E6R]RP-27	RLRLPRIARPVPEVLPARLPLPALPRN	12.14	-0.28
[E1R,E6R,E13R]RP-27	RLRLPRIARPVPRVLPARLPLPALPRN	13.28	-0.24
[A8W]RP-27	ELRLPEIWRPVPEVLPARLPLPALPRN	10.72	-0.29
[A8W,A17W]RP-27	ELRLPEIWRPVPEVLPWRLPLPALPRN	10.72	-0.22
[A8W,A17W,A23W]RP-27	ELRLPEIWRPVPEVLPWRLPLPWLPRN	10.72	-0.14

pI represents the calculated isoelectric point and GRAVY represents the Grand Average of
Hydropathy.

2.2. Nuclear magnetic resonance

Peptides were dissolved in 700 µL of either H_2O/D_2O (9/1 v/v) or
H_2O/trifluoroethanol-d_3 (TFE-d_3; 1/1 v/v) at a final concentration of 2.5 mM. The methyl
resonance of TSP-d_4 (~1 mM) was used as internal reference both for ^{1}H and ^{13}C chemical
shift scale. NMR spectra were recorded at 300°K with a Unity Inova 500NM high-resolution
spectrometer (Agilent Technologies, CA, USA) operating at a ^{1}H frequency of 500 MHz,
equipped with an indirect detection probe. [1]H spectra were acquired using a 6.1 µs pulse
(90°), 3 s delay time, 1.5 s acquisition time and a spectral width of 8 kHz. The WET
sequence [13,14] was applied to suppress the water signal (100 Hz wide uburp shape centered
at water resonance). 2D experiments, namely, [1]H-^{1}H gradient correlation spectroscopy
(gCOSY), [1]H-^{1}H double-quantum filtered COSY (dqfCOSY), [1]H-^{1}H total correlation

spectroscopy (TOCSY) and ^{1}H-^{1}H nuclear Overhauser effect spectroscopy (NOESY) were acquired over the same spectral window, sampling each of the 512 increments (256 for gCOSY) with 2048 complex points and 48 scans. Mixing time was 80 and 200 ms for the TOCSY and NOESY, respectively. The ^{1}H-^{13}C gradient heteronuclear single-quantum correlation (gHSQC) spectra were acquired using a spectral width of 8 kHz and 21 kHz for ^{1}H and ^{13}C, respectively.

2.3. NMR-based structure calculation

3D structures of peptides were obtained by combining the simulated annealing algorithm implemented in the NMR molecular dynamics and analysis system DYNAMO [15] and experimentally derived restraints. Scalar coupling constants between ^{1}H$_N$ and ^{1}H$_\alpha$ within the same residue were measured and related to the Φ backbone torsion angle through the Karplus equation [16]. Only J-coupling values lower than 6 Hz or larger than 8 Hz were considered, in order to avoid overinterpretation of values lying in the dynamic average range. NOESY cross-peaks (NOEs) were classified on the basis of their relative intensity as strong, medium and weak, and upper limits of 0.27, 0.33 and 0.50 nm were applied, respectively, to restrain the corresponding inter-proton distances. Only unambiguously assigned NOEs were considered. A harmonic potential was applied to the potential energy above the upper limit, while contribution was zero otherwise.

A statistical analysis was performed on the ^{1}Hα, ^{1}Hβ, ^{13}Cα and ^{13}Cβ chemical shift values with the software TALOS+ [17]. Briefly, TALOS+ takes the peptide sequence as input and analyses it in terms of successive (i-1, i, i+1) residue triplets. For each of these, the ten best-matched triplets are searched in a high-resolution structure database by comparing both the experimental chemical shift values provided and the residue types. In parallel, the

prediction output of the implemented artificial neural network is also compared. The final prediction of Φ/Ψ backbone torsion angles is very stringent. The prediction is ranked as valid ("good") only if the central residue of all the 10 best-matched triplets are found in the same region of the Ramachandran plot, otherwise it is designated as ambiguous ("warn"). In addition, if a random coil index (RCI) order parameter $S2$ is predicted to be less than 0.5, the residue is categorized as "dynamic" and no value for either Φ and Ψ is considered during structure calculations [18,19]. In the present work, only the "good" predictions were used as torsional angles restraints.

1000 structures were calculated with 5k steps at 4000^oK and 20k steps of cooling down to zero. Solvent molecules were not included in the calculations. The 100 conformers with the lowest potential energy were selected for the analysis. Among the latter, the conformer with the minimum average root mean square deviation (RMSD) from all the others was selected as representative (cluster centroid). Then, all successive RMSD calculations were performed by using this representative structure as reference. In order to calculate the backbone bending angle at the site of residue E13, we calculated the minimum angle between two vectors, whose tail and head point were obtained as the centre of gravity of the backbone atoms of selected residues as follows: 13, 12 and 11 (vector 1 tail); 10 and 9 (vector 1 head); 13, 14 and 15 (vector 2 tail); 16 and 17 (vector 2 head).

2.4. Effects on cytokine production

Experiments were performed on cells collected from the peritoneal cavities of unstimulated 8-week-old C57BL/6 mice under sterile conditions using 5 mL of cold phosphate-buffered saline as previously described [20]. Isolated cells, comprising a mixed population of immune cells with predominance of macrophages and B cells, were suspended

in Dulbecco's Modified Eagle Medium culture medium containing 10% fetal bovine serum.

Peptides (5 and 20 μg mL^{-1}) were incubated with cells (2 x 10^5 cells/well) for 24 h at 37°C in

three independent incubations with 5- 6 mice per group. After incubation, cell-free

supernatants were collected and kept at -20°C until time of analysis. Concentrations of tumor

necrosis factor-alpha (TNF-α), interleukin-1β (IL-1β) and interleukin-10 (IL-10) were

determined in triplicate using ELISA Duosets from R & D Systems (Minneapolis, MN, USA)

according to manufacturer's recommended protocols.

2.5. *Insulin release studies using BRIN-BD11 cells*

BRIN-BD11 rat clonal β-cells were seeded into 24-well plates and allowed to attach

during overnight incubation at 37 °C. Incubations with purified synthetic peptides (10^{-12} - 3

x10^{-6} M, n = 8) were carried out for 20 min at 37°C in Krebs-Ringer bicarbonate (KRB)

buffer supplemented with 5.6 mM glucose as previously described [21]. After incubation,

aliquots of cell supernatant were removed for insulin radioimmunoassay [22]. Control

incubations were carried out in parallel with the well-established insulin stimulatory agents

10 mM alanine and 10 nM human glucagon-like peptide-1 (GLP-1). In order to investigate

the effects of the peptides on the integrity of the plasma membrane, peptides (10^{-7} - 3 x 10^{-6}

M; n = 4) were incubated with BRIN-BD11 cells for 20 min 37°C and the rate of lactate

dehydrogenase (LDH) release was measured using a CytoTox 96 non-radioactive cytotoxicity

assay kit (Promega, Southampton, UK) according to the manufacturer's instructions as

previously described [21].

2.6.   Insulin release studies using mouse islets

The preparation of isolated pancreatic islets from adult, male National Institutes of Health NIH Swiss mice (Harlan Ltd, Bicester, UK) and the procedure for determining the effects of peptides on the rate of insulin release has been described previously [24]. The islets were incubated for 1 h at 37°C with RP-27 in KRB buffer supplemented with 16.7 mM glucose. Control incubation with GLP-1 (10^{-8} and 10^{-6} M), 10 mM alanine, and KRB buffer containing 16.7 mM glucose alone were carried out in parallel. Supernatants were removed for determination of insulin concentration by radioimmunoassay. The islet cells were retrieved and extracted with acid-ethanol to determine total insulin content as previously described [23].

2.7. Statistical analysis

The distributions of data were evaluated for normality using Kolmogorov-Smirnov test and then retested with Chi-Square test. Comparison of quantitative parametric data between two study groups was done by application of unpaired t-test. Differences between the paired data were evaluated using paired t-test or Mann-Whitney test as appropriate. A P-value of < 0.05, was considered statistically significant.

3. Results

3.1. NMR-based structure calculation.

Resonance assignments of RP-27 in H_2O/D_2O (9:1 v/v) and H_2O/TFE-d_3 (1:1 v/v) are reported in Tables S1 and S2, respectively. Fig. S1 shows the two corresponding ^{1}H-NMR spectra. Significant difference in the resonance positions can clearly be seen. This is particularly evident for the H_N resonances between 7.5 and 9.0 ppm, which are also spread over a larger frequency range in the presence of 50% v/v TFE (0.56 and 0.85 ppm in 0% and 50% TFE, respectively), indicating that the level of structuration increased with TFE addition. The statistical analysis performed with TALOS+ on the measured chemical shifts of both ^{1}H and ^{13}C indicated no well-defined secondary structure even in the presence of TFE. Nevertheless, while residues from positions 2 to 6 and from 17 to 26 were predicted to be part of the peptide's flexible regions in water, in the presence of TFE the backbone angles were predicted to be more restricted for the entire sequence. While the number of residues in the PP-II region is the same in water and in 50% TFE-water, in the latter solvent we found an increased number of residues in the right-handed portion of the Ramachandran plot. On the basis of TALOS+ results, backbone torsion angles were restrained for only 40% of the amino acid residues in water, while the restraints were included for up to 80% of the residues in the presence of TFE. As far as the dipolar contacts are concerned, only sequential NOEs were identified in both the solvents. In particular, strong 1H-1H dipolar interactions were observed only between the Hα of the ith-residue and the HN of the ith+1-residue. In water, a total of only 12 inter-proton distance restraints were included in the structure calculations, while up to 20 inter-proton distances were restrained in the presence of TFE. Almost all the ${}^3J_{HN-H\alpha}$

coupling constants were found in the 6-8 Hz range (Tables S1 and S2) which is typically observed for unstructured or very flexible peptides [24].

The Ramachandran plots obtained from the analysis of the 100 structures with the minimum potential energy out of the one thousand calculated through DYNAMO are shown in Fig.1. Both torsions and inter-nuclear distances were restrained during the calculations on the basis of the NMR results. Both the distribution and the standard deviation bars obtained in aqueous solution were larger than in the presence of 50% TFE-water, clearly showing a more defined peptide conformation. In water, all the proline residues (Fig.1A, red data points) appeared to be almost identical, sharply populating the PP-II region of the Ramachandran plot except for residue P5 which is located at the beginning of the peptide sequence. As expected, proline residues showed more restricted plasticity compared with the other amino acids as can be seen by the smaller standard deviation bars in both the Φ and Ψ dimensions. On the other hand, the leucine residues (Fig.1A, blue data points) show very large standard deviation bars in the Φ dimension. This suggests that there is a significant probability of finding the leucine residues in the left-handed helical region of the plot which is quite unusual for residues other than glycine. It is worth noting that all the leucine residues are located on the N-terminal side of one proline residue. The only exception is L2, whose large standard deviation bars is explained by its localization at the very beginning of the peptide sequence. In addition, only two other residues with Φ error bars exceeding the center of the plot were found, namely, R9 and R26. While the latter is located at the very end of the peptide sequence, R9 is located on the N-terminal side of one proline. Finally, we found 6 non-leucine and non-proline residues in the PP-II region of the Ramachandran plot, which in addition to the 6 out of 7 prolines makes a total of 12 residues with backbone angles typical of a PP-II conformation.
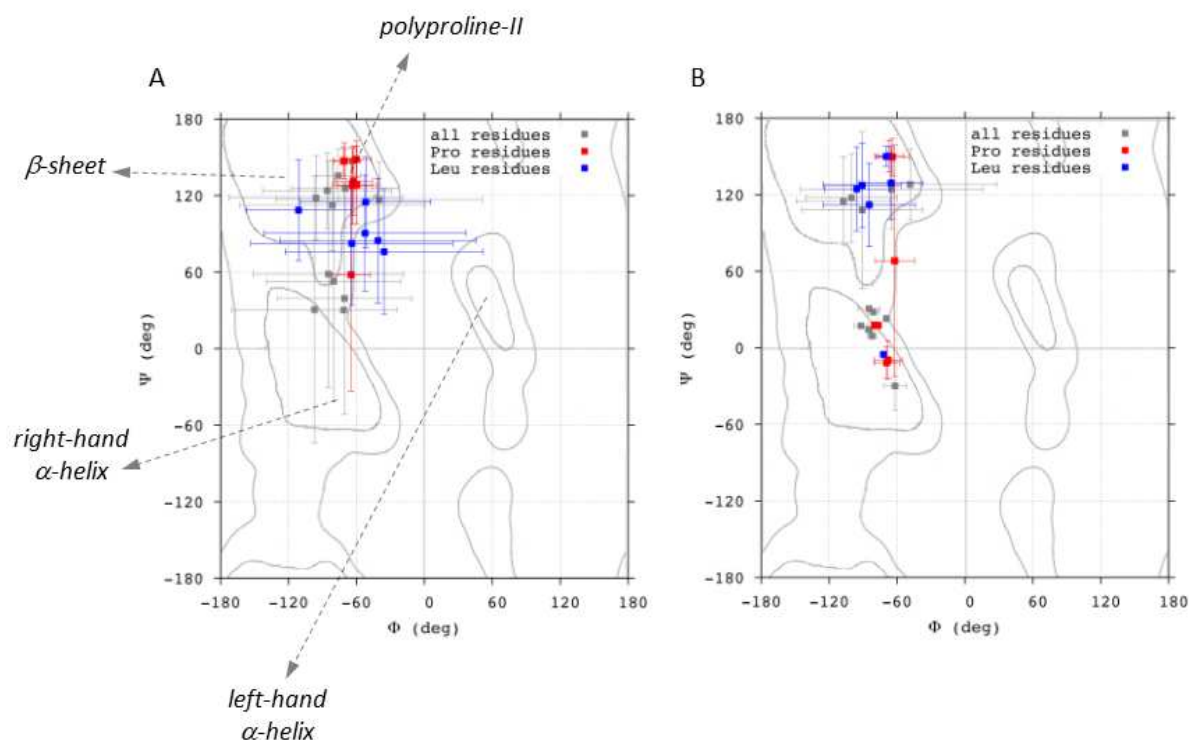
12

Fig. 1. Ramachandran plot of RP-27 in (A) $H_2O:D2O$ 9:1 v/v and (B) H_2O/TFE d3 1:1 v/v. The most energy-favored regions are reported according to Lovell et al. [25].

In 50% TFE-water, the amino acid residues appeared to be well segregated into two distinct regions of the plot, namely the PP-II and a region corresponding to a not well-defined, right-handed helical conformation with about 3 residues per turn. Major differences from the results obtained in water are: (A) only 2 proline residues are found in the PP-II region, and (B) almost all leucine residues moved to the PP-II region. Residues populating the helical region are grouped in short and separated portions along the peptide sequence, namely, residues 2-3, 5-7, 12-13, 16 - 18, and 22-23. This implies that the peptide conformation is characterized by numerous and abrupt changes from right-handed to left-handed coils proceeding from the N-terminus to the C-terminus. While the number of

residues in the PP-II region is the same in water and in 50% TFE-water, in the latter solvent we found an increased number of residues in the right-handed portion of the Ramachandran plot.

The 3D view of the backbone trace of the 100 conformers obtained with the lowest potential energy in the two solvents is shown in Fig. 2. The RMSD was calculated by using the cluster centroid as reference. When the RMSD was calculated on the basis of the alignment performed over almost the entire peptide sequence (Figs. 3A and C), the lowest value was obtained in 50% TFE-water, indicating lower plasticity in this solvent. However, the difference was not dramatic, as shown by the standard deviations obtained, making the two proposed conformations quite comparable. In both cases, a clear bend was observed at the site of residue Glu[13] separating two linear extended portions up to residues 9 and 18. Consequently, structure alignment was also performed over the region from Arg[9] to Arg[18] in order to visualize better the bend (Figs. 3B and D). RMSD results confirmed the lower plasticity in 50% TFE-water. The bending angle of the backbone was estimated to be $120 \pm 23°$ in water and $99 \pm 23°$ in 50% TFE-water.
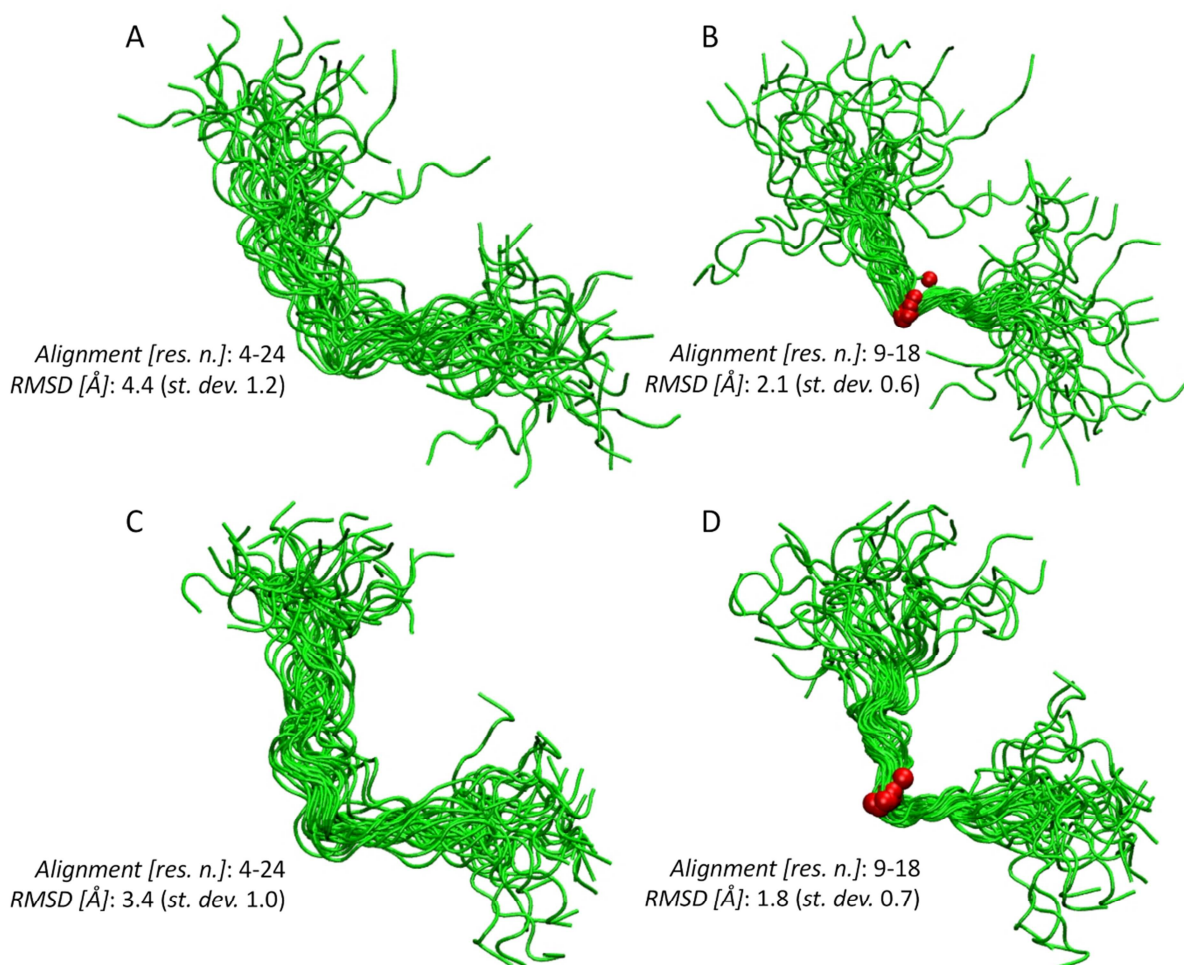
Fig. 2. Backbone trace (3D view) of the 100 conformers with the lowest potential energy obtained for RP-27 in $H_2O:D_2O$ (9:1 v/v) (panels (A and B) and H_2O:TFE d3 (1:11 v/v) (panels C and D). Conformers were aligned on the basis of two different portions of the sequence, namely residues 4 to 24 (A and C) and residues 9 to 18 (B and D). The corresponding mean values of the backbone RMSD from the cluster centroid with the standard deviation in parentheses are reported. The red spheres in panels B and D represent the alpha carbon of residue E13.

3.2. *Effects on cytokine production*

Incubation of mouse peritoneal cells with RP-27 at a concentration of 5 µg/mL (approx. 1.5 nM) significantly ($P < 0.05$) increased production of the anti-inflammatory cytokine IL-10 (Fig. 4A) and inhibited production of the pro-inflammatory cytokines TNF-α

15

(Fig. 4B) and IL-1β (Fig. 4C). RP-33 inhibited the production of TNF-α only (Fig. 4B).

Increasing cationicity of the peptide by the substitution Glu^1→ Arg abolished the effects of

the peptide on TNF-α, IL-1β and IL-10 production at both 5 µg/mL and 20 µg/mL

concentrations. Increasing cationicity further by the additional substitution Glu^6→ Arg had

no significant effect on TNF-α production but restored the ability of RP-27 to inhibit

production of IL-1β and enhance production of IL-10 at the concentration of 20 µg/mL. The

ability to stimulate significantly IL-10 production as well as inhibit IL-1β production was

restored in the very strongly cationic tri-substituted analogue [E1R,E6R,E13R]RP-27

(calculated pI 13.28) but the peptide was without effect on TNF-α production at 5 µg/mL and

20 µg/mL concentrations. The tryptophan-containing analogues of RP-27 ([A8W]RP-27 and

[A8W,A17W]RP-27) did not show any significant effect on the production of TNF-α, IL-1β

and IL-10 when tested in doses of 5 and 20 µg/mL. The strongly hydrophobic tri-substituted

analogue [A8W,A17W,A23W]RP-27 significantly increased IL-10 production at the

concentration of 20 µg/mL while inhibition of TNF-α production was observed at the
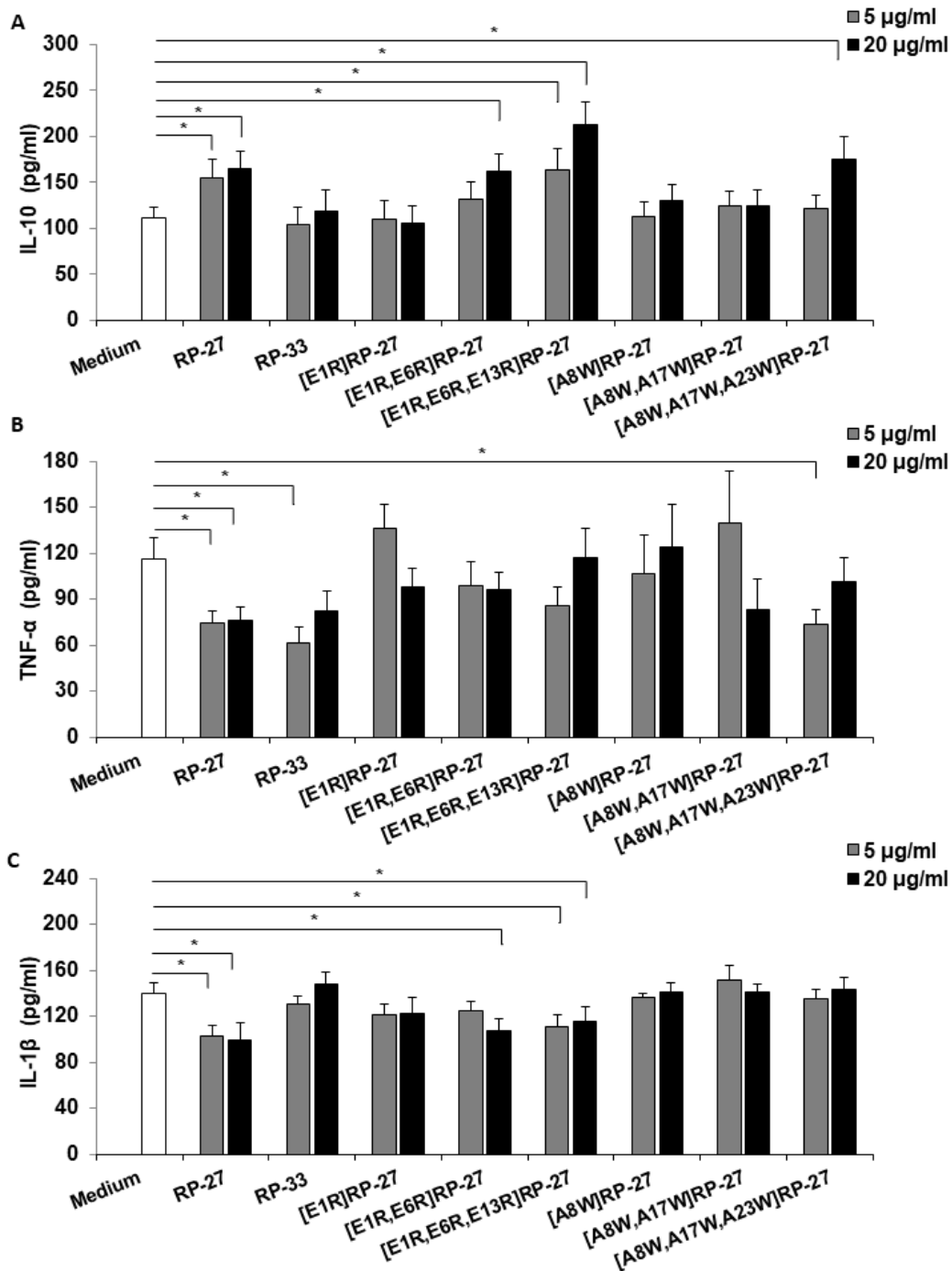
concentration of 5 µg/mL.

Fig. 3. Effects on the production of (A) IL-10, (B) TNF-α and (C) IL-1β by peritoneal cells from unstimulated C57BL/6 mice by rhinophrynin-27 and it analogs (5 µg/mL and 10 µg/mL). * P < 0.05 compared to cytokine production in medium only.

17

3.4. Effects on insulin release by BRIN-BD11 cells

In the presence of 5.6 mM glucose alone, the rate of release of insulin from BRIN-BD11 clonal β-cells was 0.69 ± 0.02 ng/10^6 cells/20 min. RP-27 produced a concentration-dependent increase in the rate of insulin release (Fig. 4). The threshold concentrations (minimum concentrations of peptide producing a significant ($P < 0.05$) increase in insulin release compared with 5.6 mM glucose alone) was 1 nM. At the highest concentration tested (3 µM), the peptide produced an approximately 3-fold increase in the rate of insulin release. At concentrations up to and including 3 µM, incubation with RP-27 had no effect upon the rate of release of the cytosolic enzyme lactate dehydrogenase demonstrating that the integrity of the plasma membrane of the cells had been preserved. The effects of substitution of the glutamic acid residues in RP-27 by arginine and substitution of the alanine residues by tryptophan are summarized in Table 2. The substitution $Glu^1 \rightarrow Arg$ in RP-27 resulted in a decrease in insulinotropic potency (threshold concentration 10 nM) and further substitutions by arginine in the [E1R,E6R] and [E1R,E6R,E13R] analogues resulted in loss of activity at concentrations up to and including 3 µM. RP-33 and all tryptophan-containing peptides lacked insulinotropic activity at concentrations up to and including 3 µM (Table 2).
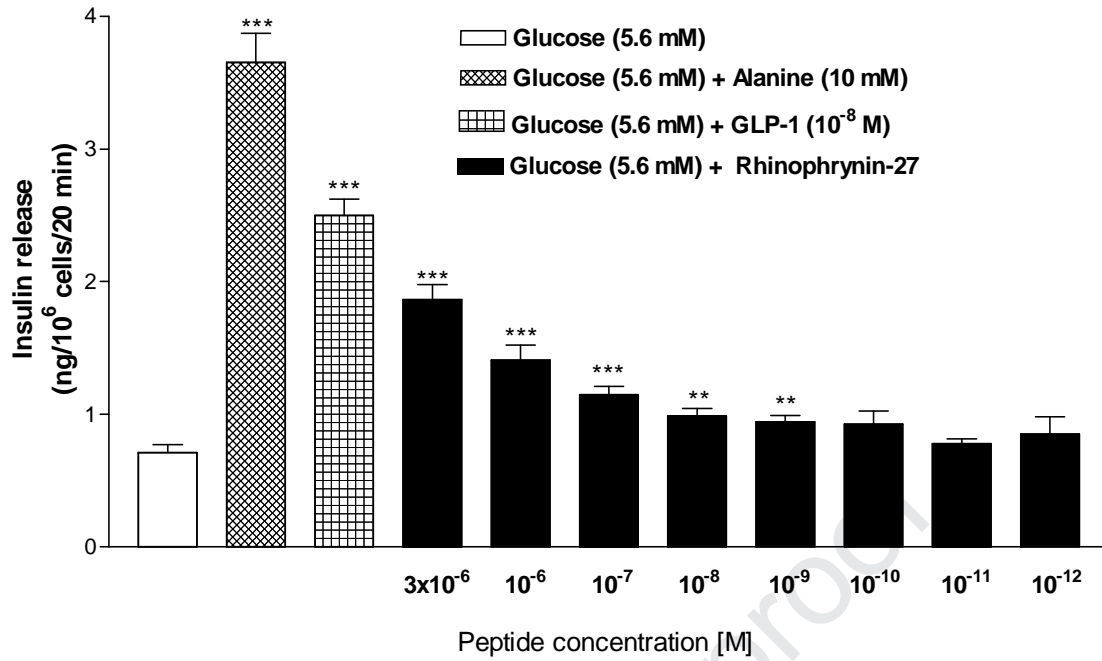
Fig. 4. Effects of increasing concentrations of rhinophryrin-27 on the release of insulin from BRIN-BD11 clonal β-cells. ** P < 0.01, ***P < 0.001 compared with release in the presence of 5.6 mM glucose alone.

Table 2. Effects of rhinophrynin-27 and its analogues on the rate of insulin release from

BRIN-BD11 clonal β-cells

Peptide	Threshold Conc. (M)	Max. effect
None	NA	100
RP-27	10^{-9}	273 ± 6 *
RP-33	$>3 \times 10^{-6}$	100 ± 3
[E1R]RP-27	10^{-8}	173 ± 5*
[E1R,E6R]RP-27	$>3 \times 10^{-6}$	102 ± 4
[E1R,E6R,E13R]RP-27	$>3 \times 10^{-6}$	100 ± 4
[A8W]RP-27	$>3 \times 10^{-6}$	101 ± 7
[A8W,A17W]RP-27	$>3 \times 10^{-6}$	107 ± 2
[A8W,A17W,A23W]RP-27	$>3 \times 10^{-6}$	108 ± 3

Threshold concentration refers to the minimum concentration of peptide producing a

significant increase in the rate of insulin release compared with the rate in the presence of

glucose only. Max. effect refers to % increase in the rate of insulin release in the presence of

3 μM peptide compared with the rate in the presence of 5.6 mM glucose alone (100%). NA:

not applicable, *P < 0.001 compared with 5.6 mM glucose alone.

20

3.5. Effect on insulin release by mouse pancreatic islets

The rate of insulin release from mouse islets in the presence of 16.7 mM glucose control was 7.7 ± 1.2 % of the total insulin content of the islets released in 60 min. RP-27 at 1µM concentration produced a significant ($P < 0.01$) increase in the rate of insulin release compared with the rate with glucose only (Fig. 5) The effect of 1 µM RP-27 (12.9 ± 0.7% of total insulin released in 60 min) was significantly less than that produced by 1 µM GLP-1 (17.5 ± 2.4 % of total insulin released in 60 min).
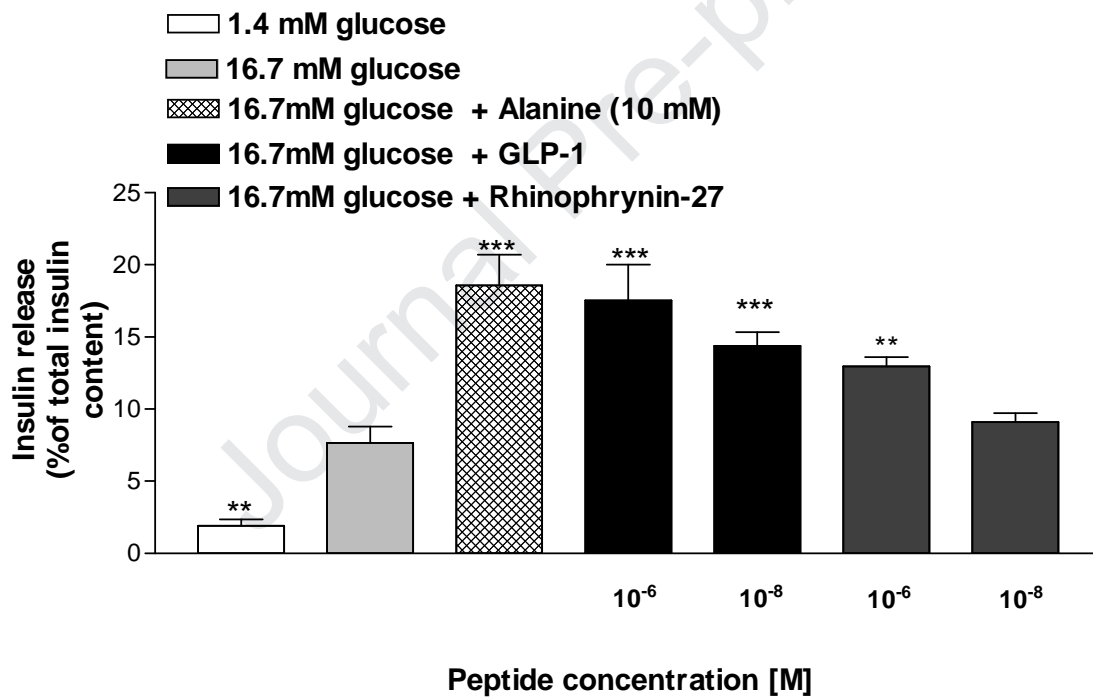

Fig. 5. Effects of rhinophryrin-27 on the release of insulin from isolated mouse islets.

** $P < 0.01$, ***$P < 0.001$ compared with release in the presence of 5.6 mM glucose alone.

4. Discussion

Skin secretions from the Mexican burrowing toad *R. dorsalis*, in common with frogs from the genus *Pipa* but unlike those from *Xenopus*, *Hymenochirus*, and *Pseudhymenochirus* (Pipidae), do not contain cationic, α-helical host-defense peptides with antimicrobial properties [2]. This observation led to suggestion that the ability to produce such peptides by frogs within the Pipidae family arose in the common ancestor of (*Hymenochirus* + *Pseudhymenochirus*) + *Xenopus* after divergence from the line of evolution leading to extant *Pipa* species [2]. However, *R. dorsalis* secretions do contain the non-cytotoxic peptide RP-27 whose biological activities and functional role are completely unknown. Orthologous peptides have not been found in skin secretion of members of the Pipidae family studied to-date [9,26].

Both in water and in the presence of 50% TFE-water, RP-27 adopts an extended conformation with a marked bend at the site of E13. The distribution of the backbone Φ/Ψ angles on the Ramachandran plot (Fig. 1) supports the previous interpretation of the circular dichroism spectra [2]. In water, the strong negative band at 200 nm was taken as indicative of a type II polyproline (PP-II) helical structure, and the absence of the characteristic positive, although small, band expected at 220 nm was attributed to deviation from the ideal PP-II conformation. The PP-II structure was also suggested on the basis of a small shift of the negative band from the wavelength typical for unordered structures (195 nm) and supported by the large number of proline residues in the RP-27 sequence. In the present work, in addition to the proline residues, we found around 50% of the residues in the PP-II region of the Ramachandran plot (Fig. 1A), with the majority of the other amino acids localized in left-handed coil regions. These results confirm that, in water, RP-27 adopts a general PP-II-like

22

conformation with a high degree of deviation from the canonical collagen-like folding and high plasticity.

In 50% TFE-water, we found a similar situation with the same number of residues located in the PP-II region of the Ramachandran plot, although the number of proline residues in this region decreased (Fig. 1B). Plasticity was clearly reduced in this solvent and the amino acid residues were well separated in two groups, namely PP-II and right-handed coil (3 residues per turn). The increased proportion of residues in right-handed coils was probably responsible for the increased intensity of the negative band at about 225 nm in the circular dichroism spectrum [2]. An overall extended structure was obtained, very similar to the one obtained in water, with a marked bend at the site of residue E13. The angle of this bend was smaller in the presence of TFE but the difference with the structure obtained in water was rather small, when the standard deviation is taken into consideration. Our study indicates that the overall structure of RP-27 in solution is only slightly influenced by the presence of TFE, which acts to stabilize a particular conformation that was already well established in water. When RP-27 sequence is compared to the canonical PP-II helix in collagen, the amino-acid pattern is quite different. The collagen primary structure is characterized by -G-x-y- repetitive triplets, where x and y are often P residues. In the case of RP-27, two consecutive proline residues are not found and the peptide exhibits the -P-x-P-y-x-x-P-x-y-x-P-x-P- motif in the middle of the sequence (residues 10 to 22), where x and y are hydrophobic and hydrophilic residues, respectively. A particular feature of the proposed structure of RP-27 is the almost 90° bend in the middle of the sequence. An unexpected observation arising from the study was that a BLAST search revealed that RP-27 shows appreciable sequence identity to a region of a sub-unit of the trimeric MtrE outer membrane channel of bacterium *Neisseria gonorrhoeae* (Fig. S3) [27]. This small portion of

the 447 amino acid residue protein also exhibits an approximately 90° bend. The significance, if any, of these observations is unknown.

R. dorsalis is rarely seen in the wild, emerging from its underground burrow only to reproduce after the first rains [28], so that it is not readily amenable to physiological investigations. However, the observed immunomodulatory properties of RP-27 in mice may be relevant to the biological significance of the peptide in its species of origin. Both innate and adaptive immune responses are involved in the abilities of frogs to defend against infections by pathogenic microorganisms in the environment. It has been shown that macrophage activation in the skin of *Xenopus tropicalis* is a major response to infection by *Mycobacterium liflandii* leading to granulomatous inflammation [29]. The present study has shown that RP-27 inhibits the production of the pro-inflammatory cytokines TNF-α and IL-1β by mouse peritoneal cells and stimulates production of the anti-inflammatory cytokine IL-10 thereby creating a predominately immunosuppressive environment, This may serve to modulate an excessive and potentially harmful inflammatory response triggered by exposure to pathogens. A previous study has shown that the frog skin peptides tigerinin-1M, -1R and -1V, while lacking antimicrobial and hemolytic activities, significantly enhance the production of IL-10 by mouse peritoneal macrophages and human peripheral blood mononuclear cells [30]. However, immunosuppression is not a universal characteristic of frog skin-derived peptides. For example, frenatin-2D from *Discoglossus sardus* (Alytidae) [31] and plasticin-L1 from *Leptodactylus laticeps* (Leptodactylidae) [32], which like RP-27 lack antimicrobial and cytotoxic activities, stimulate production of TNF-α and IL-1β by mouse peritoneal cells.

The immunomodulatory properties of RP-27 may have clinical relevance in terms drug development. Endotoxemic complications of infection, such as severe sepsis and septic shock are a major cause of death particularly in intensive care units [33]. The importance of agents that modulate the immune function of the host in the treatment of sepsis is well

24

recognized [34] and several immunoregulatory peptides have shown therapeutic potential in attenuating the inflammatory response triggered by bacteria [35]. In view of its ability to inhibit production of TNF-α and IL-1β and stimulate IL-10 production by peritoneal cells, it will be worthwhile to investigate the ability of RP-27 to attenuate the early hyperinflammatory response that follows bacterial infection in an appropriate animal model. Such a study in a model of acute inflammation may provide additional insight into the relevance of RP-27 and analogues in experimental therapy.

Defective insulin release is a characteristic of patients with long-standing Type 2 diabetes mellitus (T2DM). Several frog skin-derived peptides show therapeutic potential for treatment of such patients by virtue of their insulinotropic activities (reviewed in [5]). These compounds generally, but not invariably, have the ability to adopt an amphipathic α-helical conformation in a membrane-mimetic solvent or in the presence of a phospholipid micelle. This study has shown that RP-27, which adopts a polyproline type II helical conformation in solution, also stimulates insulin release from rat clonal β-cells (Fig. 3) and mouse pancreatic islets (Fig. 4) at concentrations that do not increase the rate of LDH release. However, the potency and maximum response produced by the peptide were significantly less than the corresponding parameters for GLP-1. Metabolic syndrome is associated with insulin resistance, impaired glucose tolerance, high blood pressure and elevated circulating concentrations of cholesterol and triglycerides [36]. Elevated levels of TNF-α induce insulin resistance in adipocytes and peripheral tissues by impairing insulin signalling [37]. Another critical event in the pathogenesis of T2DM is IL-1β-mediated autoinflammation followed by β-cell death [38]. Neutralization of IL-1β or blockade of its receptor has showed beneficial effects on the restoring of β-cell function and even regeneration of islets [39]. Consequently, blocking TNF-α and IL-1β production by RP-27 in conjunction with its ability to stimulate

IL-10 production and insulin release may represent part of an effective strategy for preventing the progression of metabolic syndrome into T2DM.

Attempts to increase the insulinotropic potency and/or effectiveness of RP-27 or its ability to modulate cytokine production by synthesis of selected analogs were disappointing. Increasing cationicity by progressive substitutions of glutamic acid residues by arginine and increasing hydrophobicity by progressive substitutions of alanine residues by tryptophan resulted in peptides that showed either decreased activity or were inactive (Table 2). The mechanism of action of RP-27 is unknown at this time and it seems highly improbable that cells from laboratory rodents would contain a specific receptor for a frog peptide with very restricted distribution. The speculation arises that RP-27 is binding to a receptor whose natural ligand is mammalian peptide that adopts a stable polyproline type II helical conformation. This structural feature occurs frequently in proteins and is believed to have an important functional role in protein-protein or protein-nucleic acid interactions and recognition [40]. The observation that modification of the C-terminus of the peptide by addition of the cationic hexapeptide sequence KMAKNQ in the naturally occurring RP-33 abolishes insulin-releasing activity and the ability to inhibit production of IL-1β and IL-10 suggests that the C-terminal domain of RP-27 may be particularly important in interacting with any putative receptor. As RP-33 is present in *R. dorsalis* skin secretions in appreciably higher concentration than RP-27 [2], the data suggest the RP-33 is a biosynthetic precursor of RP-27 that is activated in the skin in response to an appropriate stimulus.

Acknowledgments

26

Author Contributions

M.A.S., P.C., J.P., and V.M. conducted the experiments. M.A.S., Y. A.-W., A.L., M.L.L. and J.M.C. designed the experiments. J.M.C. and M.A.S. wrote the manuscript. All authors read and

approved the final manuscript.

Note

Declarations of interest: none

References

[1]   D.R. Frost, Amphibian species of the world: an online reference. Version 6.0.

Electronic Database accessible at

http://research.amnh.org/herpetology/amphibia/index.html. American Museum of

Natural History, New York, USA, 2018.

[2]   J.M. Conlon, L. Guilhaudis, J. Leprince , L. Coquet, M.L. Mangoni, S. Attoub, T.

Jouenne, J.D. King, Peptidomic analysis of skin secretions of the Mexican burrowing

toad *Rhinophrynus dorsalis* (Rhinophrynidae): Insight into the origin of host-defense

peptides within the Pipidae and characterization of a proline-arginine-rich peptide,

Peptides 97 (2017) 22-28.

[3]   B. Agerberth, J.Y. Lee, T. Bergman, M. Carlquist, H.G. Boman, V. Mutt, H. Jörnvall,

Amino acid sequence of PR-39. Isolation from pig intestine of a new member of the

family of proline-arginine-rich antibacterial peptides, Eur. J. Biochem. 202 (1991) 849-

854.

[4]   J.M. Pantic I.P. Jovanovic, G.D. Radosavljevic, N.N. Arsenijevic, J.M. Conlon, M.L.

Lukic, The potential of frog skin-derived peptides for development into therapeutically-

valuable immunomodulatory agents, Molecules 22 (2017) E2071.

[5]   J.M. Conlon, M. Mechkarska, Y.H. Abdel-Wahab, P.R. Flatt. Peptides from frog skin

with potential for development into agents for Type 2 diabetes therapy, Peptides 100

(2018) 275-281.

[6]   O.O. Ojo, J.M. Conlon, P.R. Flatt, Y.H. Abdel-Wahab, Frog skin peptides (tigerinin-

1R, magainin-AM1, -AM2, CPF-AM1, and PGla-AM1) stimulate secretion of

glucagon-like peptide 1 (GLP-1) by GLUTag cells, Biochem. Biophys. Res. Commun.

431 (2013) 14-18.

[7]   V. Musale, Y.H.A. Abdel-Wahab, P.R. Flatt, J.M. Conlon, M.L. Mangoni, Insulinotropic, glucose-lowering, and beta-cell anti-apoptotic actions of peptides related to esculentin-1a(1-21).NH_2, Amino Acids 50 (2018) 723-734.

[8]   M.L. Mangoni, A.M. McDermott, M. Zasloff, Antimicrobial peptides and wound healing: biological and therapeutic considerations, Exp. Dermatol. 25 (2016) 167-173.

[9]   X. Xu, R. Lai, The chemistry and biological activities of peptides from amphibian skin secretions, Chem. Rev. 115 (2015) 1760–1846.

[10] N.H. McClenaghan, C.R. Barnett, E. Ah-Sing, Y.H.A. Abdel-Wahab, F.P.M. O'Harte, T.-W. Yoon, S.K. Swanston-Flatt, P.R. Flatt, Characterization of a novel glucose-responsive insulin-secreting cell line, BRIN-BD11, produced by electrofusion, Diabetes 45 (1996) 1132-1140.

[11]   L.P. Kozlowski, IPC - Isoelectric Point Calculator, Biol. Direct. 11 (2016) 55.

[12]   W.C. Wimley, S.H. White, Experimentally determined hydrophobicity scale for proteins at membrane interfaces, Nat. Struct. Biol. 3 (1996) 842-848.

[13] R. Ogg, P. Kingsley, J. Taylor, WET, a T_1- and B_1-insensitive water-suppression method for in vivo localized ^{1}H NMR spectroscopy, J. Magn. Reson., Ser. B 104 (1994) 1-10.

[14]   S. Smallcombe, S. L. Patt, P. Keifer, P. WET solvent suppression and its applications to LC NMR and high-resolution NMR spectroscopy, J. Magn. Reson., Ser. A 117 (1995) 295-303.

[15]   DYNAMO: the NMR molecular dynamics and analysis system, accessible at http://spin.niddk.nih.gov/NMRPipe/dynamo.

[16]   M. Habeck, W. Rieping, M. Nilges, Bayesian estimation of Karplus parameters and torsion angles from three-bond scalar couplings constants, J. Magn. Reson. 177 (2005) 160–166.

29

[17]   Y. Shen, F. Delaglio, G. Cornilescu, A. Bax, TALOS+: A hybrid method for

predicting protein backbone torsion angles from NMR chemical shifts, J. Biomol. NMR

44 (2009) 213-223.

[18]   M.V. Berjanskii, D.S. Wishart, A simple method to predict protein flexibility using

secondary chemical shifts, J. Am. Chem. Soc. 127 (2005) 14970-14971.

[19]   M. V. Berjanskii, D.S. Wishart, Application of the random coil index to studying

protein flexibility J. Biomol. NMR 40 (2008) 31-48.

[20] J. M. Pantic, M. Mechkarska, M.L. Lukic, J.M. Conlon, Effects of tigerinin peptides on

cytokine production by mouse peritoneal macrophages and spleen cells and by human

peripheral blood mononuclear cells, Biochimie 101 (2014) 83-92.

[21]   B.O. Owolabi, V. Musale, O.O. Ojo, R.C. Moffett, M.K. McGahon, T.M. Curtis, J.M.

Conlon, P.R. Flatt, Y.H.A. Abdel-Wahab, Actions of PGLa-AM1 and its [A14K] and

[A20K] analogues and their therapeutic potential as anti-diabetic agents, Biochimie

138, (2017) 1-12.

[22]   P.R. Flatt, C.J. Bailey, Abnormal plasma glucose and insulin responses in

heterozygous lean (ob/+) mice, Diabetologia 20 (1981) 573-577.

[23]   G.V. Graham, J.M. Conlon, Y.H. Abdel-Wahab, P.R. Flatt, Glucagon-related peptides

from phylogenetically ancient fish reveal new approaches to the development of dual

GCGR and GLP1R agonists for type 2 diabetes therapy, Peptides 110 (2018) 19-29.

[24]   J. Cavanagh, W.J. Fairbrother, A.G. Palmer, M. Rance, N.J. Skelton, Protein NMR

Spectroscopy - Principles and Practice, 2nd edition. Elsevier Academic Press, Oxford,

UK.

(25)   S. C. Lovell, I. W. Davis, W. B. Arendall, P. I. W. de Bakker, J. M. Word, M. G.

Prisant, J. S. Richardson, D. C. Richardson, Structure validation by Calpha geometry:

phi,psi and Cbeta deviation, Proteins 50 (2003) 437–450.

[26]   J.M. Conlon, M. Mechkarska, Host-defense peptides with therapeutic potential from skin secretions of frogs from the family Pipidae, Pharmaceuticals (Basel) 7 (2014) 58-77.

[27]   H. T. Lei, T.H., Chou, C.C. Su, J.R. Bolla, N. Kumar, A. Radhakrishnan, F. Long, J.A. Delmar, S.V. Do, K.R. Rajashankar, W.M. Shafer, E.W. Yu, Crystal structure of the open state of the *Neisseria gonorrhoeae* MtrE outer membrane channel. Plos One 2014, 9, e97475.

[28]   G. Santos-Barrera, G. Hammerson, F. Bolaños, G. Chaves, L.D. Wilson, J. Savage, G. Köhler, *Rhinophrynus dorsalis*, The IUCN Red List of Threatened Species (2010) e.T59040A11873951.

[29]   J.J. Fremont-Rahl, C. Ek, H.R.Williamson, P.L. Small, J.G. Fox, S. Muthupalani, *Mycobacterium liflandii* outbreak in a research colony of *Xenopus* (*Silurana*) tropicalis frogs, Vet. Pathol. 48 (2011) 856-867.

[30]   J.M. Pantic, M. Mechkarska, M.L. Lukic, J.M. Conlon, Effects of tigerinin peptides on cytokine production by mouse peritoneal macrophages and spleen cells and by human peripheral blood mononuclear cells, Biochimie 101 (2014) 83-92.

[31]   J.M. Conlon, M. Mechkarska, J.M. Pantic, M.L. Lukic, L. Coquet, J. Leprince, P.F. Nielsen, A.C. Rinaldi, An immunomodulatory peptide related to frenatin 2 from skin secretions of the Tyrrhenian painted frog *Discoglossus sardus* (Alytidae), Peptides 40 (2013) 65-71.

[32]   M.A. Scorciapino, G. Manzo, A.C. Rinaldi, R. Sanna, M. Casu, J.M. Pantic, M.L. Lukic, J.M. Conlon, Conformational analysis of the frog skin peptide, plasticin-L1 and its effects on the production of proinflammatory cytokines by macrophages, Biochemistry 52 (2013) 7231-7241.

[33]   S. Jain, Sepsis: An update on current practices in diagnosis and management, Am. J.

       Med. Sci. 356 (2018) 277-286.

[34]   R.S. Hotchkiss, G. Monneret, D. Payen, Immunosuppression in sepsis: a novel

       understanding of the disorder and a new therapeutic approach. Lancet Infect. Dis. 13

       (2013) 260-268.

[35]   K.Y. Choi, L.N. Chow, N. Mookherjee, Cationic host defence peptides: multifaceted

       role in immune modulation and inflammation, J. Innate Immun. 4 (2012) 361-370.

[36]   S. O'Neill, L. O'Driscoll, Metabolic syndrome: a closer look at the growing epidemic

       and its associated pathologies, Obes. Rev. 16 (2015) 1-12.

[37]   M.S.H. Akash, K. Rehman, A. Liaqat, Tumor necrosis factor-alpha: role in

       development of insulin resistance and pathogenesis of Type 2 diabetes mellitus, J. Cell.

       Biochem. 119 (2018) 105-110.

[38]   C.A. Dinarello, M.Y. Donath, T. Mandrup-Poulsen, Role of IL-1beta in type 2

       diabetes, Curr. Opin. Endocrinol. Diabetes Obes. 17 (2010) 314-321.

[39]   L. Adorini, Cytokine-based immunointervention in the treatment of autoimmune

       diseases, Clin. Exp. Immunol. 132 (2003) 185-192.

[40]   A.A. Adzhubei, M.J. Sternberg, A.A. Makarov, Polyproline-II helix in proteins:

       structure and function, J. Mol. Biol. 425 (2013) 2100-2132.

Research Highlights

- In water and 50% TFE-water, RP-27 adopts a polyproline type II helical conformation.

- The conformation contains a marked bend at the site of E13.

- RP-27 inhibited production of TNF-α and IL-1β and stimulated production of IL-10.

- RP-27stimulated release of insulin from BRIN-BD11 clonal β-cells at concentrations ≥ 1 nM.

BIOCHIMIE conflict of interest declaration and author agreement form

Title of Paper: Conformational analysis and in vitro immunomodulatory and insulinotropic properties of the frog skin host-defense peptide rhinophrynin-27 and selected analogs

Author (s): Mariano A. Scorciapino, Paola Carta, Jelena Pantic, Miodrag L. Lukic, Aleksandra Lukic, Vishal Musale , Yasser H.A. Abdel-Wahab, J. Michael Conlon

Please delete one of the following two lines:
We have no conflict of interest to declare.

This statement is to certify that all Authors have seen and approved the manuscript being submitted, and agree to the submission to *BIOCHIMIE*. We warrant that the article is the Authors' original work. We warrant that the article has not received prior publication, is not under consideration for publication elsewhere, and will not be submitted for publication elsewhere, in whole or in part, while under consideration for publication in *BIOCHIMIE*. On behalf of all Co-Authors, the corresponding Author shall bear full responsibility for the submission.

We attest to the fact that all Authors listed on the title page have contributed significantly to the work, have read the manuscript, attest to the validity and legitimacy of the data and their interpretation, and agree to its submission to *BIOCHIMIE*. We further attest that no other person has fulfilled the requirements for authorship as stated in the Elsevier Authorship-factsheet (2017_ETHICS_AUTH02 - attached), but is not included in the list of authors, and that no other person has contributed substantially to the writing of the manuscript but is not included either among the authors or in the acknowledgements.

All authors agree that no modification to the author list can be made without the written acceptance of all authors and the formal approval of the Editor-in-Chief. All authors accept that the Editor-in-Chief's decisions over acceptance or rejection or in the event of any breach of the Principles of Ethical Publishing in *BIOCHIMIE* being discovered, of retraction are final.

On behalf of all authors *(delete line if not appropriate)*

J. Michael Conlon

Corresponding Author Signature :

Date 10/1/2019